Food Chemistry: X 25 (2025) 102025

Contents lists available at ScienceDirect

Food Chemistry: X

journal homepage: www.sciencedirect.com/journal/food-chemistry-x

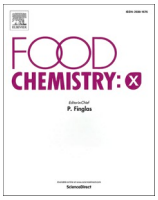

Identification and comparison of *N*-glycome profiles from common dietary protein sources

Matthew Bolino [a], İzzet Avcı [b], Hacı Mehmet Kayili [c], Hatice Duman [d], Bekir Salih [b], Sercan Karav [d], Steven A. Frese [a,e,*]

[a] *Department of Nutrition, University of Nevada, Reno, Reno, NV 89557, USA*
[b] *Department of Chemistry, Faculty of Science, Hacettepe University, 06500 Ankara, TR, Republic of Türkiye*
[c] *Department of Biomedical Engineering, Faculty of Engineering, Karabük University, 78000 Karabük, TR, Republic of Türkiye*
[d] *Department of Molecular Biology and Genetics, Çanakkale Onsekiz Mart University, 17020 Çanakkale, TR, Republic of Türkiye*
[e] *University of Nevada, Reno School of Medicine, Reno, NV 89557, USA*

ARTICLE INFO

Keywords:
N-glycan
Protein
Mass spectrometry
Microbiome
N-glycome
Glycan

ABSTRACT

The *N*-glycomes of bovine whey, egg white, pea, and soy protein isolates are described here. *N*-glycans from four protein isolates were analyzed by HILIC high performance liquid chromatography and quadrupole time-of-flight tandem mass spectrometry (HILIC-FLD-QTOF-MS/MS). In total, 33 *N*-glycans from bovine whey and egg white and 10 *N*-glycans from soy and pea glycoproteins were identified. The type of *N*-glycans per glycoprotein source were attributable to differences in biosynthetic glycosylation pathways. Animal glycoprotein sources favored a combination of complex and hybrid glycan configurations, while the plant proteins were dominated by oligomannosidic *N*-glycans. Bovine whey glycoprotein isolate contained the most diverse *N*-glycans by monosaccharide composition as well as structure, while plant sources such as pea and soy glycoprotein isolates contained an overlap of oligomannosidic *N*-glycans. The results suggest *N*-glycan structure and composition is dependent on the host organism which are driven by the differences in *N*-glycan biosynthetic pathways.

1. Introduction

Glycosylation is one of several post-translational modifications to protein after the synthesis by ribosomes. Glycosylation has a variety of responsibilities, such as protein function, stability, solubility, and structure (Molinari, 2007; Skropeta, 2009; Stanley et al., 2015). *O*-glycans are carbohydrates conjugated to serine or threonine residues and include an array of different structures found on many proteins, including mucins and mucin-like proteins found in foods (Takada et al., 2020). In contrast, *N*-linked glycans are complex carbohydrate moieties bound to asparagine residues of many cellular proteins (Fernández-Tejada et al., 2015) and secreted proteins, such as bovine milk proteins (Nwosu et al., 2012). During *N*-glycan synthesis, a 14 subunit *N*-glycan (Glc3Man9GlcNAc2) synthesized in the endoplasmic reticulum (ER) is transferred from the lipid anchor, dolichol pyrophosphate, to an asparagine residue linked *via* an *N*-acetylglucosamine within a specific *N*-glycosylation acceptor sequence (Asn-X-Ser/Thr) of the recipient protein (Bieberich, 2014). The *N*-glycan structure is then modified and "trimmed" in the ER and Golgi apparatus by hydrolytic removal of sugar residues followed by re-glycosylation or "processing" by the addition of new monomers such as galactose, fucose, or mannose, and the composition and architecture of the resulting *N*-glycan is dependent on the organism and the particular glycosylation site and/or glycoprotein (Bieberich, 2014). *N*-linked glycans act as a quality control checkpoint for proper protein folding in the ER, resulting in the export of the protein from the ER or tagging the protein for degradation (Aebi et al., 2010; Helenius & Aebi, 2004). Additionally, other cellular roles such as protein transport, migration, and adhesion have also been attributed to glycosylation (Bieberich, 2014).

N-glycans from dietary glycoproteins or derived from the host may also serve as energy substrates for the adult microbiota, especially when fiber intake is low. *N*-glycoproteins ingested from diet or shed host epithelial cells are likely the primary sources of *N*-glycans (Koropatkin et al., 2012). Among infants, *N*-glycans bound to human milk proteins can serve as important substrates for an infant gut microbe, *Bifidobacterium longum* subsp. *infantis* (*B. infantis*; Barratt et al., 2022; Karav et al., 2019; Karav, Parc, et al., 2015). For example, *B. infantis* has been shown to release *N*-glycans from human milk proteins *in vivo* (Karav

* Corresponding author at: Department of Nutrition, University of Nevada, Reno, 1664 N Virginia St, Reno, NV 89557, USA.
E-mail address: sfrese@unr.edu (S.A. Frese).

https://doi.org/10.1016/j.fochx.2024.102025
Received 27 September 2024; Received in revised form 12 November 2024; Accepted 18 November 2024
Available online 20 November 2024

et al., 2019) and access to available *N*-glycans can serve as an important fitness determinant for *B. infantis* (Barratt et al., 2022). There is also evidence that *N*-glycans can serve as prebiotics (Barratt et al., 2022; Karav et al., 2016). However, most research on the *N*-glycome of dietary protein sources has focused on bovine and human milk (Barboza et al., 2012; Dallas et al., 2011; Karav, Bell, et al., 2015; Nwosu et al., 2012; Parc et al., 2015; Smilowitz et al., 2013; Zivkovic et al., 2011), and much of the knowledge of *N*-glycan utilization by the gut microbiome has focused on individual constituent microbes (Briliūtė et al., 2019; Crouch et al., 2022).

Structural differences between human and other mammalian milk *N*-glycomes are well characterized (Barboza et al., 2012; Nwosu et al., 2012; Smilowitz et al., 2013; Zivkovic et al., 2011), but other areas of research have characterized the biosynthetic systems among a wide variety of organisms, demonstrating an incredible array of potential *N*-glycan structures arising from variations in *N*-glycan biosynthetic capabilities and regulatory networks (Stanley et al., 2015). For example, mammalian bovine milk proteins contain complex, hybrid, and oligomannose *N*-glycans (Nwosu et al., 2012) while plant protein glycosylation is primarily described as oligomannosidic *N*-glycans, with no hybrid or complex types present and the inclusion of distinct carbohydrate monomers, such as arabinose and xylose (Castilho et al., 2011; Strasser, 2016). How differences in *N*-glycan structure and composition impact the composition and function of the gut microbiome is not understood, and there is currently a paucity of knowledge as to the structural composition of dietary *N*-glycans among common sources in the diet to address this gap in knowledge. This study sought to characterize the *N*-glycan structures from four glycoproteins sources that are widely consumed in whole and processed foods; egg white (from *Gallus gallus domesticus*), bovine whey protein (from *Bos taurus*), pea (from *Pisum sativum)*, and soybean (from *Glycine max*).

2. Methods

2.1. Protein purification

Protein was purified from commercially available whey, egg, soy, and pea protein isolates derived from large-scale commodity ingredient processing in the United States. Each sample was subjected to four rounds of ethanol precipitation by adding four volumes of ice-cold ethanol, incubation at −20 °C overnight, then followed by centrifugation at 4 °C (3,270RCF, 25 min) to remove residual sugars and other remaining contaminants. The protein samples were subsequently aliquoted and dried at 30 °C under vacuum centrifugation (Eppendorf 5301 Vacufuge Concentrator System). After rehydration with distilled H_2O, the purified protein was then quantified using a Qubit BR Protein assay (ThermoFisher Scientific, Waltham, MA USA).

2.2. N-glycan deglycosylation

Initially, 0.5 mg of each sample was transferred into microcentrifuge tubes and 50 µL of 1 % SDS (Sodium Dodecyl Sulfate) was added to each sample to facilitate protein solubilization. Samples were then subjected to incubation at 70 °C with shaking at 600 rpm for 10 min. Following this, 25 µL of 4 % NP-40 (Nonidet P-40) and 25 µL of 5× PBS (Phosphate-Buffered Saline) were added and the mixture was gently vortexed to ensure thorough mixing. Subsequently, 1 U of PNGase F (Peptide N-Glycosidase F) obtained from Promega (Madison, WI, USA) was added to each sample to enzymatically release *N*-linked glycans from the glycoprotein substrates and incubated overnight at 37 °C.

2.3. N-glycan labeling

To label released *N*-glycans, 50 µL of the procainamide labeling (110 mg/mL procainamide in a 10:3 (*v/v*) mixture of DMSO (Dimethyl sulfoxide) and glacial acetic acid) and 50 µL of the $NaCNBH_3$ (Sodium cyanoborohydride, 63 mg/mL $NaCNBH_3$ in a 10:3 (*v/v*) mixture of DMSO and glacial acetic acid) were added to the entire released glycan samples and incubated at 65 °C for 2 h as described (Kayili & Salih, 2021). After the incubation period, samples were centrifuged at maximum speed (16,300 x g) for 5 min at room temperature to pellet any insoluble materials. The supernatant containing the labeled *N*-glycans was carefully transferred to fresh microcentrifuge tubes for subsequent analysis.

2.4. N-glycan purification

To purify *N*-glycans, cotton-HILIC was used as described previously (Kayili & Salih, 2021). Briefly, a cotton wool plug was inserted into a pipette tip (100 µL capacity). The cotton wool-containing pipette tip underwent a washing procedure consisting of three rinses with pure water followed by three rinses with an 85 % acetonitrile (ACN) solution. Following this, a loading solution was prepared by mixing 15 µL of procainamide-labeled *N*-glycan sample with 85 µL of ACN. Each sample (loading solution) was then aspirated and dispensed 15 times using a cotton wool-containing pipette tip. Subsequently, each cotton wool-containing pipette tip underwent a washing process comprising of five rinses with 100 µL of a solution containing 85 % ACN, 14 % water, and 1 % trifluoroacetic acid (TFA) (*v/v/v*), followed by five rinses with an 85/15 ACN/water (*v/v*) solution. Finally, the *N*-glycans that were loaded onto the cotton wool were eluted by aspirating and dispensing 10 times with 25 µL of pure water.

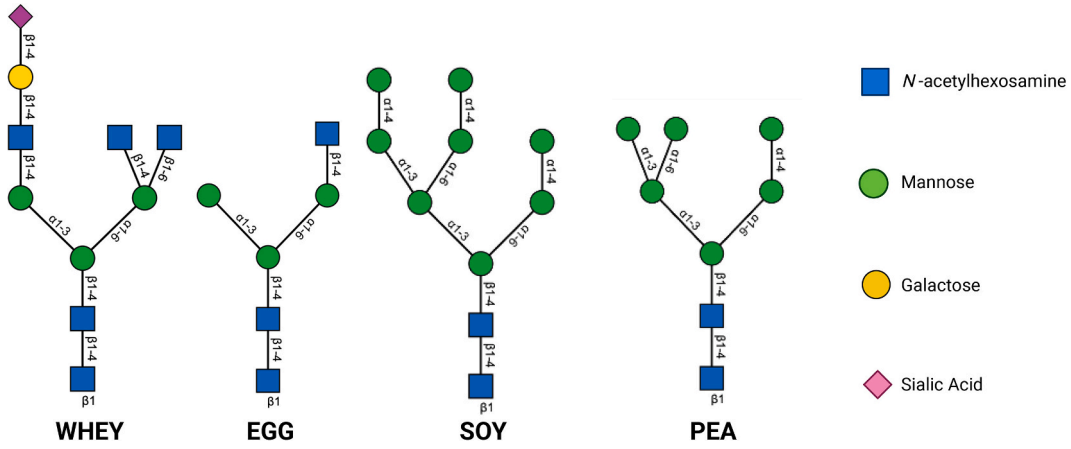

Fig. 1. The most abundant *N*-glycan structures across protein sources, as determined by mass spectrometry.

Table 1
N-glycan data from each protein source elucidated by HILIC-FLD-QTOF MS/MS.

Glycan Peak*	Composition	m/z meas.	z	m/z calc.	Δ MH+	Score	IntCov. [%]	FragCov. [%]	Rt [min]	S1 Area	S2 Area	S3 Area	S1 RelAbun	S2 RelAbun	S3 RelAbun	Average	SD	Source
1	Hex3HexNAc4-proc	768.85568	2	768.837313	−0.018367	89.8249074	92.6470588	92.6470588	22.3998833	4.1564	2.4502	7.4321	0.92073941	1.24001804	1.49777403	1.21951049	0.23601929	Bovine whey
2	Hex3HexNAc4dHex1-proc	841.88673	2	841.866267	−0.0204626	93.2546687	94.2622951	94.2622951	24.5248917	7.7333	3.7575	10.7176	1.71310607	1.90162753	2.15989329	1.92487563	0.1831394	Bovine whey
3	Hex5HexNAc2-proc	727.82821	2	727.810764	−0.0174461	91.6692608	95.7746479	95.7746479	26.08265	2.2423	0.7806	3.1389	0.49672168	0.39505268	0.6325753	0.50811655	0.09730238	Bovine whey
4	Hex4HexNAc4-proc	849.88501	2	849.863725	−0.0212853	96.1484797	101.136364	101.136364	27.0465	10.6602	4.7577	14.4384	2.36148259	2.40781725	2.90973756	2.55967913	0.24825041	Bovine whey
	Hex5HexNAc3-proc	829.3762	2	829.35045	−0.0257498	md	md	md										Bovine whey
5	Hex3HexNAc6-proc	971.93992	2	971.916686	−0.0232345	139.405646	209.638554	209.638554	28.4132	31.5604	12.2417	43.1782	6.99136369	6.19538356	8.70160337	7.29611688	1.04560678	Bovine whey
6	Hex4HexNAc4dHex1-proc	922.9165	2	922.8927	−0.0238	md	md	md	29.4	2.5224	1.0007	3.1648	0.55877035	0.50644276	0.63779487	0.56766933	0.05399221	Bovine whey
	Hex4HexNAc5-proc	951.42229	2	951.403411	−0.018879	md	md	md										Bovine whey
7	Hex6HexNAc2-proc	808.85271	2	808.837176	−0.0155344	90.327175	102.222222	102.222222	30.1532333	54.0703	19.6322	68.7391	11.9778308	9.9356306	13.8528328	11.9220981	1.5996766	Bovine whey
	Hex3HexNAc6dHex1-proc	696.98339	3	696.966185	−0.0172046	111.54972	132.903226	132.903226										Bovine whey
8	Hex4HexNAc5dHex1-proc	683.3085	3	683.2907	−0.0178	md	md	md	31.6	33.1508	13.1676	43.7383	7.34367434	6.6639709	8.81447904	7.60737476	0.89752428	Bovine whey
	Hex5HexNAc4-proc	930.90713	2	930.9176	0.01047	md	md	md	32.2									Bovine whey
9	Hex5HexNAc4dHex1-proc	669.63381	3	669.615153	−0.0186573	106.239048	116.568047	116.568047	33.2567583	21.2923	7.7321	26.9514	4.71674038	3.91312687	5.43145368	4.68710698	0.62020839	Bovine whey
10	Hex3HexNAc6dHex2-proc	1117.9958	2	1117.9746	−0.0212	md	md	md	33.9	22.8666	9.9718	24.3619	5.0654845	5.04661328	4.9095977	5.00723183	0.06946629	Bovine whey
11	Hex7HexNAc2-proc	889.8794	2	889.863587	−0.0158127	md	md	md	35.688775	104.5989	46.6089	114.4568	23.1710926	23.5882282	23.0662158	23.2751789	0.22546204	Bovine whey
	Hex4HexNAc5NeuAc1-proc	731.65619	3	731.636505	−0.019685	92.3223971	92.6553672	92.6553672										Bovine whey
12	Hex5HexNAc4NeuAc1-proc	717.98073	3	717.960989	−0.0197414	111.382305	127.81457	127.81457	36.9935	12.4948	5.9272	16.6592	2.76788922	2.99968774	3.35729027	3.04162241	0.24244214	Bovine whey
13	Hex4HexNAc5dHex1NeuAc1-proc	780.3436	3	780.3225	−0.0211	md	md	md	37.3	35.815	17.9687	35.2757	7.93385669	9.09375239	7.10903072	8.0455466	0.81409909	Bovine whey
14	Hex8HexNAc2-proc	970.9185	2	970.889999	−0.028501	md	md	md	38.554425	33.2816	16.7282	30.8663	7.37264958	8.46594961	6.22041447	7.35300455	0.91684112	Bovine whey
	Hex5HexNAc4NeuAc1dHex1-proc	766.66726	3	766.646958	−0.0203018	76.8823283	64.0449438	64.0449438										Bovine whey
15	Hex6HexNAc3NeuAc1dHex1-proc	752.9822	3	752.971442	−0.0107582	md	md	md	39.9	7.4337	3.2447	6.315	1.64673769	1.64210535	1.27264743	1.52049682	0.17526619	Bovine whey
	Hex6HexNAc5dHex1-proc	791.33758	3	791.325885	−0.0116953	md	md	md										Bovine whey
	Hex4HexNAc7NeuAc1-proc	867.0462	3	867.0228	−0.0234	md	md	md										Bovine whey
16	Hex6HexNAc4NeuAc1-proc	771.9987	3	771.9786	−0.0201	md	md	md	40.5	3.526	1.4348	1.7064	0.78109113	0.72613578	0.34388687	0.61703792	0.19444562	Bovine whey
17	Hex9HexNAc2-proc	1051.9498	2	1051.91641	−0.0333892	md	md	md	41.5	11.1146	6.2347	9.5818	2.46214278	3.15530996	1.93099812	2.51615029	0.50128001	Bovine whey
	Hex5HexNAc4NeuAc2-proc	815.0173	3	814.992794	−0.0245059	md	md	md										Bovine whey

(*continued on next page*)

Table 1 (*continued*)

Glycan Peak*	Composition	m/z meas.	z	m/z calc.	Δ MH+	Score	IntCov. [%]	FragCov. [%]	Rt [min]	S1 Area	S2 Area	S3 Area	S1 RelAbun	S2 RelAbun	S3 RelAbun	Average	SD	Source
	Hex4HexNAc7dHex1NeuAc1-proc	915.7324	3	915.7087	−0.0237	md	md	md										Bovine whey
18	Hex6HexNAc5NeuAc1-proc	839.6954	3	839.671721	−0.0236794	md	md	md	42.7	13.2418	6.9692	11.8532	2.93336712	3.52703196	2.38874814	2.94971574	0.46484619	Bovine whey
	Hex5HexNAc6NeuAc1dHex1-proc	902.0568	3	902.0332	−0.0236	md	md	md										Bovine whey
19	Hex6HexNAc5NeuAc1dHex1-proc	888.3822	3	888.3577	−0.0245	md	md	md	43.9	20.9636	9.1024	14.5264	4.64392568	4.60661994	2.92747199	4.0593392	0.80049587	Bovine whey
20	Hex6HexNAc7NeuAc1-proc	975.0518	3	975.058	0.0062	md	md	md	45.5	8.5999	3.999	2.2854	1.90507816	2.0238479	0.46057141	1.46316582	0.71059751	Bovine whey
22	Hex7HexNAc6NeuAc1-proc	961.407	3	961.3825	−0.0245	md	md	md	46.6	5.5858	2.1114	3.2683	1.2373848	1.06855525	0.65865298	0.98819768	0.24300293	Bovine whey
22	Hex7HexNAc6NeuAc1dHex1-proc	1010.0968	3	1010.0684	−0.0284	md	md	md	47.6	4.5091	1.7726	3.5545	0.99887067	0.89709247	0.71633021	0.87076445	0.11683935	Bovine whey
										451.4198	197.5939	496.2097						
1	Hex3HexNAc2-proc	1130.50043	1	1130.5086	−0.0081745	42.3473097	20.9302326	20.9302326	12.584175	375.9814	290.8445	18.38841	5.73713161	8.67280572	9.64951546	8.0198176	1.66262482	Egg white
2	Hex3HexNAc3-proc	667.29488	2	667.297627	−0.0027467	86.4858678	83.0769231	83.0769231	15.1531583	211.3544	149.0387	10.32329	3.22507446	4.4442432	5.4172572	4.36219162	0.89683355	Egg white
3	Hex3HexNAc3-proc	667.29488	2	667.297627	−0.0027467	md	md	md	md	463.5354	305.5914	20.33547	7.07312542	9.11254929	10.6712561	8.95231027	1.47329415	Egg white
4	Hex4HexNAc2-proc	646.78195	2	646.784352	−0.0024022	85.0256529	79.3103448	79.3103448	16.922525	46.2176	33.9738	2.20901	0.70523822	1.01307801	1.1592017	0.95917264	0.18920897	Egg white
5	Hex3HexNAc4-proc	768.83407	2	768.837313	−0.003243	83.5568643	83.8235294	83.8235294	18.3	775.5959	437.4663	25.27909	11.8348827	13.0449784	13.2654737	12.7151116	0.6288915	Egg white
6	Hex4HexNAc3-proc	748.32039	2	748.324038	−0.0036485	75.6937561	72.1518987	72.1518987	20.3	202.2277	111.3296	7.08162	3.08580938	3.31978082	3.71615608	3.37391543	0.26016938	Egg white
7	Hex3HexNAc5-proc	870.37341	2	870.376999	−0.0035893	88.452992	101.204819	101.204819	20.0662083	302.7415	157.878	8.01898	4.61955786	4.70782574	4.2080458	4.5118098	0.21779536	Egg white
8	Hex5HexNAc2-proc	727.80542	2	727.810764	−0.0053439	86.3200852	83.0985915	83.0985915	22.0312083	412.2976	228.82	12.9949	6.29128355	6.82327294	6.81921321	6.6445899	0.24983081	Egg white
	Hex4HexNAc4-proc	849.85808	2	849.863725	−0.0056447	94.7127525	104.166667	104.166667	22.4434									Egg white
9	Hex3HexNAc6-proc	971.91087	2	971.916686	−0.0058155	133.043624	216.86747	216.86747	22.5	413.993	199.6536	8.90533	6.3171538	5.95354867	4.67316747	5.64795664	0.70508279	Egg white
10	Hex4HexNAc4-proc	849.85808	2	849.863725	−0.0056447	md	md	md	23.3	197.8055	95.5372	5.19358	3.01833066	2.84886108	2.72538683	2.86419286	0.12008419	Egg white
11	Hex4HexNAc5-proc	951.39482	2	951.403411	−0.008591	90.4909472	110.810811	110.810811	24.0856833	375.9883	185.22	9.74813	5.7372369	5.52314751	5.11543582	5.45860674	0.25791895	Egg white
	Hex3HexNAc6-proc	971.91087	2	971.916686	−0.0058155	md	md	md	24.5									Egg white
12	Hex5HexNAc3-proc	829.34297	2	829.35045	−0.0074802	84.1287681	78.2608696	78.2608696	24.2862	16.6095	9.6779	0.49704	0.25344575	0.28858908	0.26082707		0.01513005	Egg white
13	Hex4HexNAc5-proc	951.39482	2	951.403411	−0.008591				25.7	9.484	4.0054	0.35377	0.14471715	0.11943859	0.1856446	0.14993345	0.02727901	Egg white
14	Hex3HexNAc7-proc	1073.44728	2	1073.45637	−0.0090918	122.974133	194.680851	194.680851	26	67.0606	21.1394	0.67556	1.0232833	0.63036402	0.35450736	0.66938489	0.27441731	Egg white
15	Hex4HexNAc6-proc	1052.93308	2	1052.9431	−0.0100172	106.886538	130.708661	130.708661	26.0960083	721.9209	309.4971	17.67922	11.0158514	9.22901489	9.27736039	9.84074222	0.83116202	Egg white
	Hex6HexNAc2-proc	808.83046	2	808.837176	−0.0067156	116.61876	149.350649	149.350649	26.487525									Egg white
16	Hex5HexNAc4-proc	930.88132	2	930.890136	−0.0088164	83.5445781	92.8571429	92.8571429	27.4	717.4858	309.3453	16.75076	10.9481758	9.2244883	8.79014105	9.65426838	0.93195554	Egg white

(*continued on next page*)

Table 1 (*continued*)

Glycan Peak*	Composition	m/z meas.	z	m/z calc.	Δ MH+	Score	IntCov. [%]	FragCov. [%]	Rt [min]	S1 Area	S2 Area	S3 Area	S1 RelAbun	S2 RelAbun	S3 RelAbun	Average	SD	Source
17	Hex3HexNAc8-proc	783.66134	3	783.666464	−0.0051242	120.540494	180.530973	180.530973	28.063825	240.248	102.4739	3.90663	3.66596432	3.05570924	2.05004601	2.92390652	0.66624668	Egg white
18	Hex5HexNAc5-proc	1032.42085	2	1032.42982	−0.0089727	67.7292329	82.03125	82.03125	28.8	275.323	116.4368	6.53718	4.20117667	3.47207441	3.43045535	3.70123548	0.35391989	Egg white
19	Hex4HexNAc7-proc	769.98444	3	769.990948	−0.0065078	82.1770522	101.360544	101.360544	28.8849167	3.8501	2	0.27039	0.058749	0.05963878	0.14189005	0.08675928	0.03898504	Egg white
20	Hex4HexNAc7-proc	769.98444	3	769.990948	−0.0065078	md	md	md	30.2	17.396	7.2516	0.61037	0.26544702	0.21623829	0.32029821	0.26732784	0.04250309	Egg white
21	Hex7HexNAc2-proc	889.857	2	889.863587	−0.0065873	109.002451	135.294118	135.294118	30.947225	113.1453	46.9617	3.19597	1.72649359	1.40036927	1.67711955	1.60132747	0.14352142	Egg white
22	Hex4HexNAc8-proc	837.6786	3	837.6841	−0.0055	md	md	md	32.1	305.3325	117.7066	4.89583	4.65909414	3.50993907	2.56913933	3.57939085	0.85463265	Egg white
23	Hex6HexNAc5-proc	742.63573	3	742.639915	−0.0041851	87.5368604	115.328467	115.328467	33	144.9131	54.0133	2.6528	2.21124111	1.61064369	1.39208526	1.73799002	0.34633018	Egg white
24	Hex5HexNAc7-proc	824.0032	3	824.0085	−0.0053	md	md	md	33.5	23.0876	5.3978	0.13833	0.35229562	0.16095911	0.07259015	0.19528163	0.11673992	Egg white
25	Hex5HexNAc7-proc	824.0031	3	824.0085	−0.0054	md	md	md	34.3	4.5159	1.199	0.06487	0.0689085	0.03575345	0.03404123	0.04623439	0.01604824	Egg white
26	Hex5HexNAc8-proc	891.69567	3	891.70168	−0.0060098	59.6105383	65.1162791	65.1162791	34.71845	3.6994	1.17	0.16884	0.05644945	0.03488869	0.0886006	0.05997958	0.02206942	Egg white
27	Hex5HexNAc8-proc	891.69567	3	891.70168	−0.0060098	md	md	md	35.3	83.8493	36.4603	2.00233	1.27946348	1.08722392	1.05074415	1.13914385	0.10033242	Egg white
28	Hex6HexNAc5NeuAc1-proc	839.66652	3	839.671721	−0.0052006	59.3201755	76.9230769	76.9230769	36	7.6699	3.1935	1.19681	0.11703565	0.09522822	0.62803889	0.28010092	0.24619032	Egg white
29	Hex4HexNAc7NeuAc1-proc	921.0348	3	921.0403	−0.0055	md	md	md	36.5	7.7983	3.5004	0.07403	0.11899491	0.10437979	0.03884804	0.08740758	0.03485133	Egg white
30	Hex4HexNAc8NeuAc1-proc	988.7269	3	988.7335	−0.0066	md	md	md	37.9	12.346	6.7395	0.4145	0.18838865	0.20096778	0.21751332	0.20228992	0.0119268	Egg white
										6553.4735	3353.5226	190.56304						
1	Hex3HexNAc2Pen1-proc	631.77344	2	631.77907	−0.0056298	73.3081352	58.974359	58.974359	15.2315	14.9869	18.9912	0.49082	1.09388568	1.47170689	1.21565747	1.26041668	0.15745847	Soy
2	Hex4HexNAc2-proc	646.7796	2	646.784352	−0.0047522	76.963657	65.5172414	65.5172414	17.2631167	2.3014	3.404	0.08558	0.16797793	0.26379008	0.21196358	0.2145772	0.03915878	Soy
3	Hex3HexNAc3Pen1-proc	733.31254	2	733.318756	−0.0062161	56.3748737	37.9310345	37.9310345	18.1446917	0.6812	0.8664	0.01416	0.04972042	0.06714093	0.03507133	0.05064423	0.01310865	Soy
4	Hex4HexNAc2Pen1-proc	712.79961	2	712.805482	−0.0058716	57.4349498	38.3928571	38.3928571	19.5222167	2.38	3.604	0.08556	0.17371491	0.27928891	0.21191405	0.22163929	0.04364557	Soy
5	Hex3HexNAc4Pen1-proc	834.85177	2	834.858442	−0.0066724	53.0139869	38.28125	38.28125	20.93245	0.4533	0.5365	0.04233	0.03308612	0.04157561	0.10484247	0.05983473	0.03201344	Soy
6	Hex5HexNAc2-proc	727.80521	2	727.810764	−0.0055539	78.6771012	71.8309859	71.8309859	21.626125	17.5953	21.936	0.49524	1.28427138	1.69991166	1.22660487	1.40359597	0.21084528	Soy
7	Hex6HexNAc2-proc	808.83069	2	808.837176	−0.0064856	102.426942	122.077922	122.077922	26.2726333	154.8226	167.7347	4.08861	11.3004174	12.9984579	10.1266233	11.4751662	1.1789151	Soy
8	Hex7HexNAc2-proc	889.85668	2	889.863587	−0.0069073	99.354378	113.72549	113.72549	30.5361	322.0689	310.0138	8.83872	23.5076339	24.0242557	21.8916425	23.1411773	0.90837861	Soy
9	Hex8HexNAc2-proc	970.88176	2	970.889999	−0.008239	113.198681	147.933884	147.933884	34.462275	835.7041	746.8951	25.51449	60.9975878	57.8800003	63.1940024	60.6905302	2.1802703	Soy
10	Hex9HexNAc2-proc	1051.90787	2	1051.91641	−0.0085408	100.306845	121.527778	121.527778	37.5826583	19.0672	16.4383	0.71935	1.39170456	1.27387207	1.781678	1.48241821	0.21700759	Soy
										1370.0609	1290.42	40.37486						
1	Hex3HexNAc2Pen1-proc	631.7741	2	631.7791	−0.005	69.8	55	55	15.28	9.3	5.47	0.22	2.13	3	1.62	2.31	0.57	Pea
2	Hex4HexNAc2-proc	646.7785	2	646.7844	−0.0059	77.2	64	64	16.93	3.63	1.56	0.07	0.83	0.86	0.49	0.67	0.17	Pea

(*continued on next page*)

Table 1 (*continued*)

Glycan Peak*	Composition	m/z meas.	z	m/z calc.	Δ MH+	Score	IntCov. [%]	FragCov. [%]	Rt [min]	S1 Area	S2 Area	S3 Area	S1 RelAbun	S2 RelAbun	S3 RelAbun	Average	SD	Source
3	Hex3HexNAc3Pen1-proc	733.3125	2	733.3188	−0.0062	56.4	38	38	18.14	2.83	1.66	0.03	0.65	0.91	0.19	0.55	0.3	Pea
4	Hex4HexNAc2Pen1-proc	712.7988	2	712.8055	−0.0066	66.5	49	49	19.52	3.73	1.93	0.07	0.85	1.06	0.51	0.79	0.23	Pea
5	Hex3HexNAc4Pen1-proc	834.8518	2	834.8584	−0.0067	53	38	38	20.93	2.71	1.48	0.05	0.62	0.81	0.34	0.58	0.19	Pea
6	Hex5HexNAc2-proc	727.804	2	727.8108	−0.0067	83.6	78	78	21.58	34.66	14.79	0.94	7.94	8.12	6.85	7.49	0.56	Pea
7	Hex6HexNAc2-proc	808.8315	2	808.8372	−0.0057	112.4	140	140	26.39	196.16	80.8	4.7	44.94	44.38	34.12	39.25	4.97	Pea
8	Hex7HexNAc2-proc	889.8561	2	889.8636	−0.0075	113.5	142	142	30.6	77.49	32.11	2.44	17.76	17.64	17.68	17.66	0.05	Pea
9	Hex8HexNAc2-proc	970.8821	2	970.89	−0.0079	md	md	md	35	90.01	35.69	4.03	20.62	19.61	29.26	24.43	4.33	Pea
10	Hex9HexNAc2-proc	1051.9074	2	1051.9164	−0.009	md	md	md	38	15.94	6.57	1.23	3.65	3.61	8.95	6.28	2.51	Pea
										436.4492	182.0484	13.77856						

md, manually determined; S1-S3; Sample 1, Sample 2, and Sample 3; RelAbun, Relative Abundance; *, Peaks of structural isomers are grouped together with discrete area values noted where detected.

2.5. HPLC-HILIC-FLD-QTOF-MS/MS analysis of N-glycans

Analysis of procainamide-labeled *N*-glycans was performed as described (Kayili, 2020) on a QTOF (TIMSTOF) mass spectrometer (Bruker Daltonik, GmbH) coupled with an Agilent 1200 series HPLC system featuring a fluorescence detector. Separation of the labeled *N*-glycans were achieved with a Waters Glycan BEH Amide column (2.5 µm, 2.1 mm ID x 15 cm L). The fluorescence detector was set with excitation and emission wavelengths of 310 nm and 370 nm, respectively. Mobile phases consisted of 100 % acetonitrile (Solution A) and 50 mM ammonium formate (pH: 4.4) (Solution B). A gradient elution method was employed, starting from 75 % Solution A and ending at 53 % Solution A over 60 min, with a flow rate of 0.35 mL min^{-1}. Prior to injection, 25 µL of purified procainamide-labeled *N*-glycans were mixed with 75 µL of ACN to optimize loading conditions. A 40 µL portion of this mixture was injected for analysis. Instrument control was managed using Hystar 4.1 software (Bruker Daltonik, GmHB). MS conditions included a capillary voltage of 4.5 kV, a source temperature of 250 °C, nebulizer gas set at 1.7 bar, and drying gas flow at 6 L min^{-1}. MS spectra were acquired within the range of 50 to 2800 *m/z* at a frequency of 1 Hz. MS/MS experiments targeted the two most abundant precursor ions, with spectra rates ranging from 0.5 Hz to 2 Hz. Collision energies varied depending on precursor charge states, with specific values assigned for doubly, triply, and quadruply charged precursors. Stepping-energy experiments utilized a basic stepping mode with collision Radio Frequency (RF) values set at 1500 and 2100 peak-to-peak Voltage (Vpp) (each for 50 % of the time). The detection by fluorescence and mass spectrometry was performed in parallel using a T-connection, allowing simultaneous analysis by both methods.

2.6. Data analysis

The identification of procainamide-labeled *N*-glycans was conducted using Protein Scape software V4 (Bruker Daltonik, GmHB). Initially, data from the HILIC-FLD-QTOF-MS/MS analysis was converted to .xml file format using Data Analysis software (Bruker Daltonik, GmbH). Converted data was then processed within Protein Scape. To determine *N*-glycan structures, the tandem mass spectra of procainamide-labeled *N*-glycans was searched against the GlycoQuest Search Engine. The search parameters included MS and MS/MS tolerances set to 20 ppm and 0.05 Da, respectively, with CarbBank as the database (Doubet & Albersheim, 1992). A threshold score of 10 was applied to identify the procainamide-labeled *N*-glycans. In addition, extracted ion chromatograms of the *m/z* ratio of precursors were generated, and their structures were subsequently annotated manually. Glycoworkbench was used for the illustration of *N*-glycan structures (Ceroni et al., 2008). The study was conducted with three experimental replicates, enhancing the reliability and reproducibility of the results.

2.7. Diversity and data analyses

Glycan relative abundances were used to calculate the Shannon Entropy (Shannon, 1948) and the number of observed features, as well as the Bray Curtis distance metric as a measure of beta diversity (Bray & Curtis, 1957). Bray Curtis distances were compared using an adonis PERMANOVA test for group significance (Anderson, 2001; Dixon, 2003). Alpha diversity results were compared using the nonparametric Kruskal-Wallis test (Kruskal & Wallis, 1952).

3. Results

3.1. Elucidated N-glycan structures across glycoproteins

HPLC-HILIC-FLD-QTOF-MS/MS analysis revealed a total of 33, 33, 10, and 10 *N*-glycan structures from bovine whey, egg, soy, and pea protein isolates, respectively. Interestingly, the *N*-glycans released from

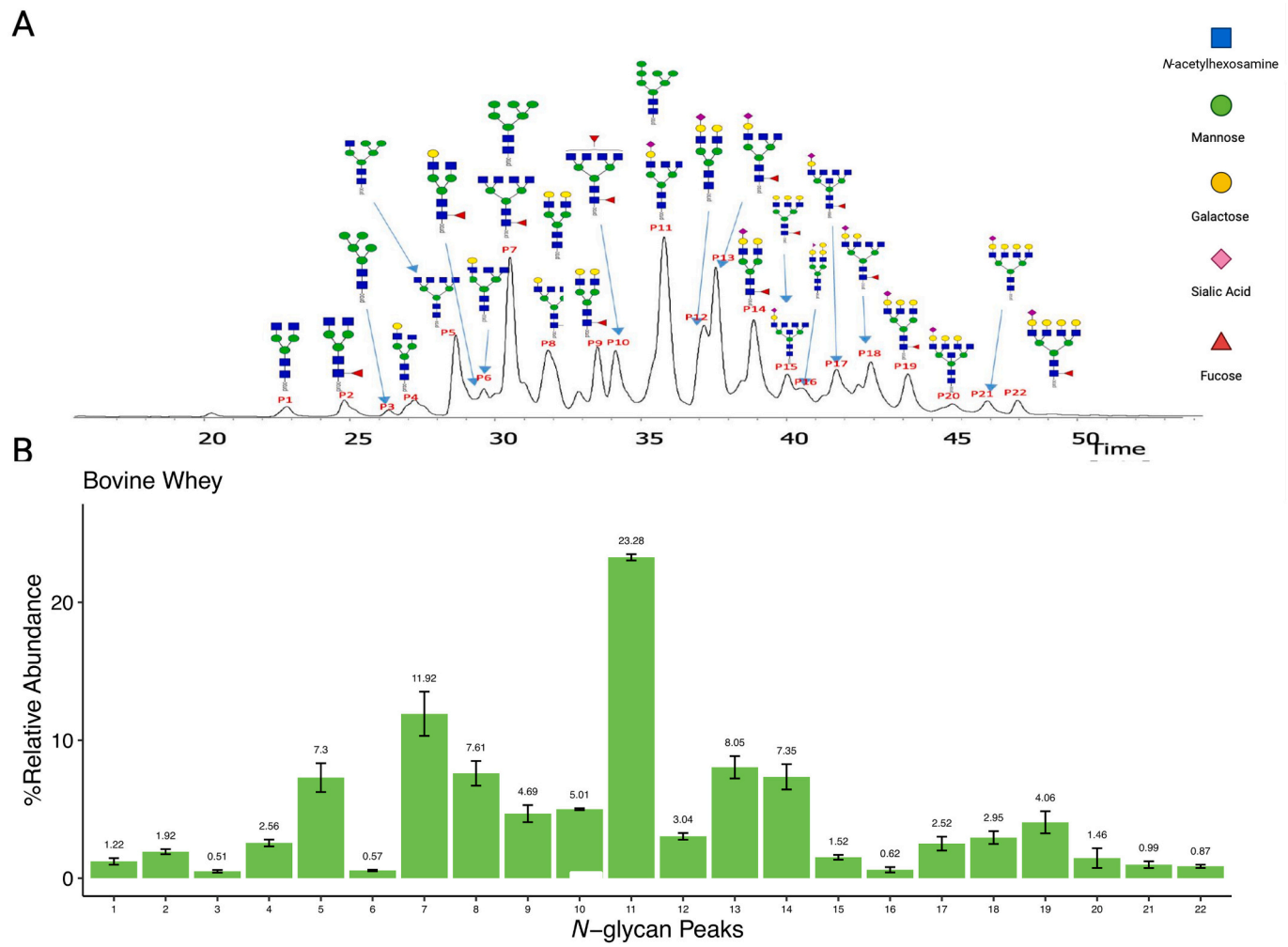

Fig. 2. Distinct *N*-glycan structures from bovine whey glycoprotein and their relative abundance determined by peak areas from the FLD chromatogram. HILIC-HPLC with a fluorescence detector paired with QTOF-MS/MS produced chromatograms then determined structures and abundance for procainamide-labeled *N*-glycans from bovine whey protein. A total of 22 peaks were identified corresponding to 33 distinct *N*-glycan structures. *N*-glycan structures for low abundant peaks not shown.

animal-sourced proteins generally had a greater number of distinct *N*-glycans, which were predominantly complex neutral and complex acidic, when compared to the plant sources. 33 *N*-glycan structures found in both bovine whey and egg white were identified, while only 10 distinct *N*-glycans for both soy and pea proteins were found and these were predominantly oligomannosidic. The most abundant *N*-glycan per protein source were distinct compared to each other, shown in Fig. 1. Table 1 shows a list of all the *N*-glycans represented by all four chromatograms with their *m/z* values, charges, relative abundances, and their glycoprotein sources.

QTOF-MS/MS identified 22 peaks, which resulted in 33 total *N*-glycan structures for bovine whey. Bovine whey contained the most diverse *N*-glycans by monosaccharide composition with 5 distinct sugars, including *N*-acetylhexoosamine (HexNAc), mannose, galactose, fucose, and *N*-acetylneuraminic acid (Neu5Ac) (Fig. 2). Bovine whey protein was the only protein that contained acidic *N*-glycans, with a total of 12 acidic structures out of the 33 total structures identified. Bovine whey also contained *N*-glycans decorated with fucose monosaccharides unlike the other protein sources, which did not contain any fucose decorations. The most abundant *N*-glycan represented 23.28 % of the total *N*-glycome of bovine whey, with the second and third most abundant *N*-glycans at 11.92 % and 8.05 %, respectively.

With similarities to the bovine whey protein in terms of the number of distinct *N*-glycan structures, QTOF-MS/MS identified 30 peaks representing 33 *N*-glycan structures for egg white protein. The monosaccharide composition decorating the egg white *N*-glycome was compromised of *N*-acetylhexosamine, mannose, and galactose with no acidic *N*-glycans present (Fig. 3). The three most abundant egg white *N*-glycans were nearly evenly distributed at 12.72 %, 9.84 %, and 9.65 %, respectively.

Unlike both animal protein sources, soy protein contained 10 peaks representing 10 distinct *N*-glycans which were predominantly oligomannosidic structures (Fig. 4). Unique to soy protein, 60.69 % of the *N*-glycome was represented by the most abundant *N*-glycan. The second and third most abundant *N*-glycans made up 23.14 % and 11.48 %, respectively. These top 3 most abundant structures made up over 90 % of soy's *N*-glycome.

Similar to the soy *N*-glycome, QTOF-MS identified 10 peaks corresponding to 10 distinct *N*-glycans that were predominantly oligomannosidic which decorated pea protein (Fig. 5). Pea protein contained a more even distribution of *N*-glycans compared to soy protein, with the most abundant structures representing 39.25 % of the *N*-glycome. The second and third most abundant structures represented 24.43 % and 17.66 % of the *N*-glycome, respectively.

3.2. *N*-glycome comparison between animal and plant sources

Consistent with the literature, we found stark differences in *N*-glycan

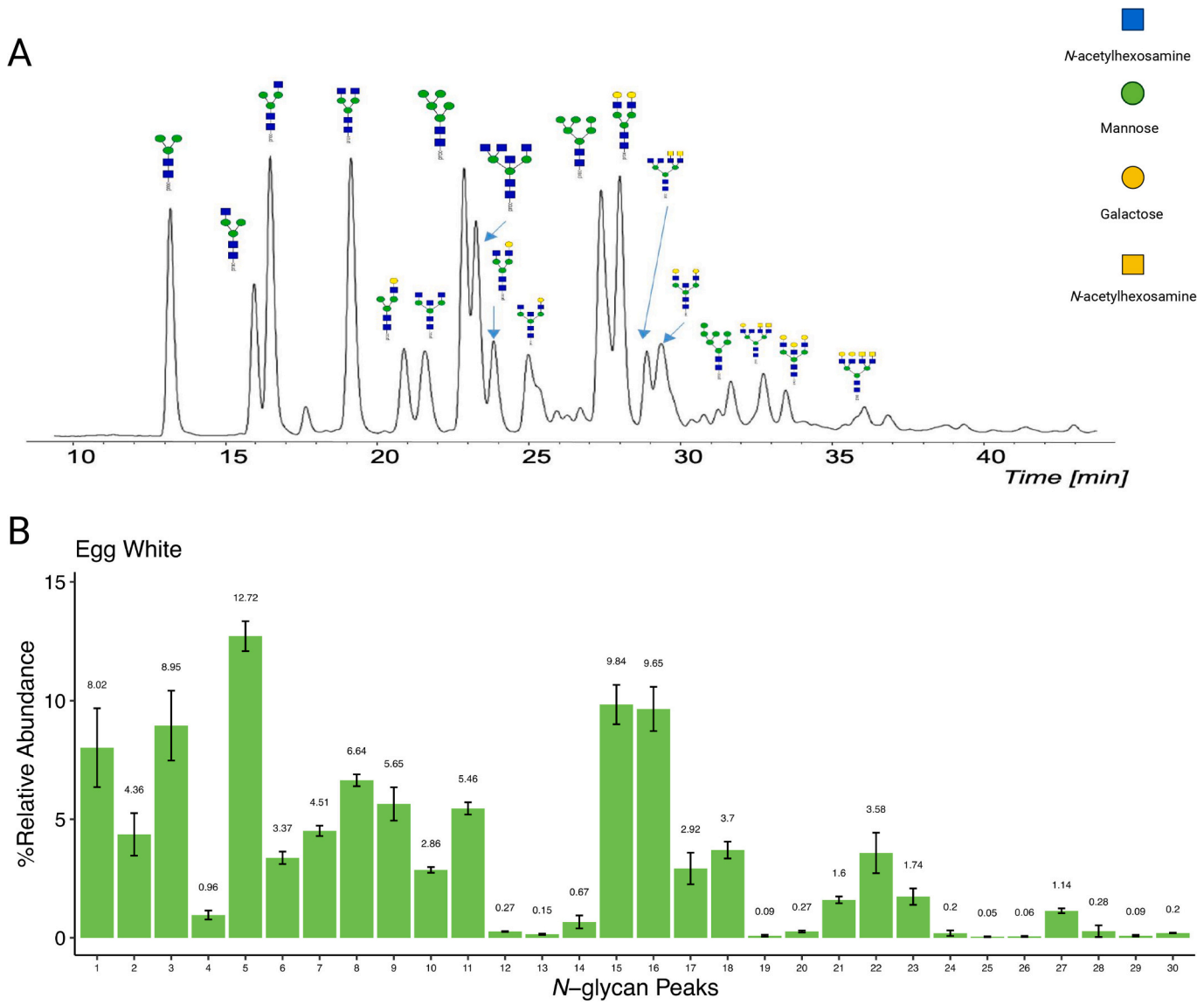

Fig. 3. Distinct *N*-glycan structures from egg white glycoprotein and their relative abundance determined by peak areas from the FLD chromatogram. HILIC-HPLC with a fluorescence detector paired with QTOF-MS/MS produced chromatograms then determined structures and abundance for procainamide-labeled *N*-glycans from egg white protein. A total of 30 peaks were identified corresponding to 33 distinct *N*-glycan structures. *N*-glycan structures for low abundant peaks not shown.

monosaccharide composition, or *N*-glycan "type" between the animal and plant sources. While the animal sources contained oligomannosidic *N*-glycans, the predominant *N*-glycan type found within both sources were complex *N*-glycans composed of multiple monosaccharide types. This is in contrast to the plant sources' *N*-glycomes, which were exclusively oligomannosidic *N*-glycan types. Interestingly, both animal sources contained roughly 20 additional structures compared to the plant sources, revealing the increased *N*-glycan diversity among the animal sources compared to the plant sources. Among all protein sources, bovine whey glycoprotein shared 11 (21 %) *N*-glycan structures with egg white protein and 5 (10 %) with both soy and pea protein, and included 20 (38 %) unique structures (Fig. 6A). The pea and soy *N*-glycome included 10 structures, which were shared (Fig. 6A), though the abundance of each *N*-glycan differed between the plant proteins (Figs. 4, 5). Finally, the egg white *N*-glycome shared 4 (8 %) structures with both the pea and soy *N*-glycomes, while containing 14 (27 %) unique *N*-glycan structural compositions (Fig. 6A), which included 7 pairs of structural isomers (Table 1). 3 (6 %) *N*-glycan structures were shared among all glycoprotein sources (Fig. 6A). When comparing animal- and plant-derived *N*-glycans, 6 *N*-glycan structures (12 %) were shared, with 42 (81 %) and 4 (8 %) unique *N*-glycan structures found within the animal sources and plant sources, respectively (Fig. 6B).

3.3. Glycan diversity and similarity

When the number of structures and their distribution among samples were compared, egg white and whey protein had the most diverse *N*-glycans by both diversity measures (Fig. S1A). When the protein sources were grouped by their source type (*e.g.*, animal *vs.* plant), the protein sources were also significantly different. Both the β-diversity measure and α-diversity measures (Shannon entropy and Observed features) were significantly different ($P = 0.002$, $P < 0.005$, and $P < 0.001$, respectively; Fig. S1B).

Egg white and whey protein had a mean Shannon entropy of 4.31 (± 0.024 SD) and 4.34 (±0.059 SD) respectively, while pea and soy protein had a mean Shannon entropy of 2.26 (±0.039 SD) and 1.59 (± 0.064 SD), respectively. For both observed features and Shannon entropy measures, the differences between group comparisons were significant ($P < 0.001$ and $P < 0.005$, respectively). The β-diversity comparisons for these *N*-glycoproteins also demonstrated significant differences when

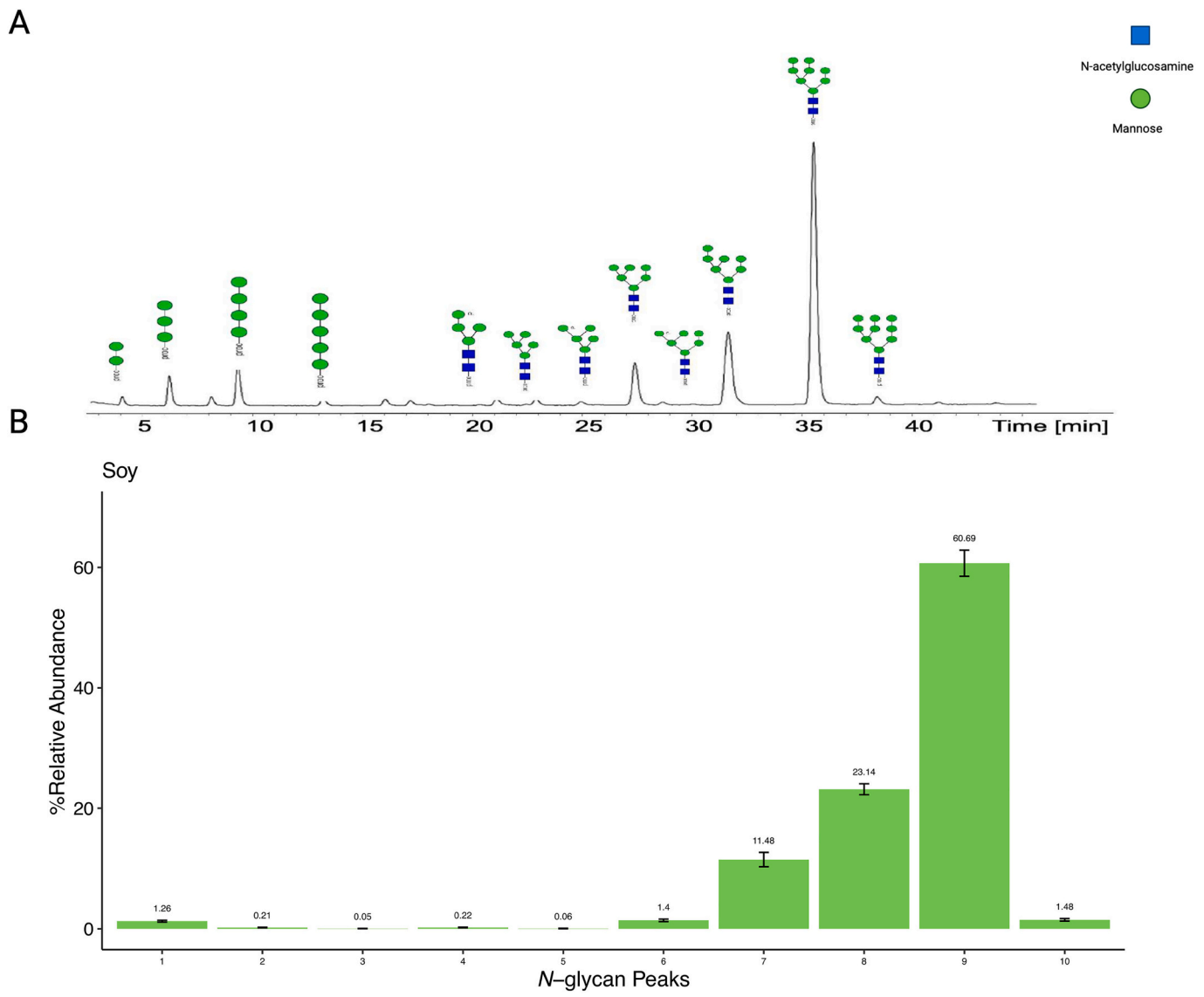

Fig. 4. Distinct *N*-glycan structures from soy glycoprotein and their relative abundance determined by peak areas from the FLD chromatogram. HILIC-HPLC with a fluorescence detector paired with QTOF-MS/MS produced chromatograms and determined structures and abundance for procainamide-labeled *N*-glycans from soy protein. A total of 10 peaks were identified corresponding to 10 distinct *N*-glycan structures. *N*-glycan structures for low abundant peaks not shown.

compared by a PERMANOVA test ($P = 0.001$).

4. Discussion

Here, we used HPLC-HILIC-FLD-QTOF-MS/MS to analyze four distinct and widely consumed sources of dietary glycoproteins from phylogenetically diverse and commercially important sources. These protein sources represent four of the most abundant sources of dietary protein among both whole and processed foods, as well as supplemental dietary protein (Smeuninx et al., 2020). We characterized the structural differences in *N*-glycans between these glycoprotein sources. HPLC-HILIC-FID-QTOF-MS/MS analysis was used to ensure proper separation, purification, and identification of complex pools of *N*-glycans.

In all, a total of 33, 33, 10, and 10 *N*-glycan structures were identified from bovine whey, egg, soy, and pea protein isolates, respectively. The main *N*-glycome difference across protein sources is found in the composition and arrangement of monosaccharides and the number of distinct *N*-glycans per protein source. Soy and pea proteins are primarily decorated with oligomannosidic *N*-glycans, whereas egg and bovine whey proteins possess structures with a wider variety of monosaccharides (Fig. 1). *N*-glycans derived from egg protein included mannose, galactose, *N*-acetylhexosamine while bovine whey included the most complex and diverse *N*-glycans, decorated with mannose, galactose, *N*-acetylhexosamine, sialic acid, and fucose. This result was reached due to the differences in glycosylation pathways between plant and animal systems. In plants, glycoproteins are predominantly modified with oligomannosidic *N*-glycans, which have simpler structures. In contrast, animals have more complex glycosylation machinery, capable of adding a wider variety of monosaccharides (*e.g.*, fucose, galactose, sialic acid) to *N*-glycans. This diversity in monosaccharides leads to greater structural variety and a higher number of distinct *N*-glycans in animal glycoproteins compared to plant sources. Given the findings in terms of the number of distinct glycans, it is unsurprising that the diversity of structures among *N*-glycoproteins differed primarily between animal and plant-derived glycoproteins. Soy and pea glycoproteins, and their composition of primarily oligomannose structures, lacked the structural diversity that was observed among the egg white and whey proteins. These findings reflect the evolutionary origins of protein *N*-glycosylation and empirical comparisons between glycoproteins in the plant and animal kingdoms (Pedrazzini et al., 2016; Wang et al., 2017).

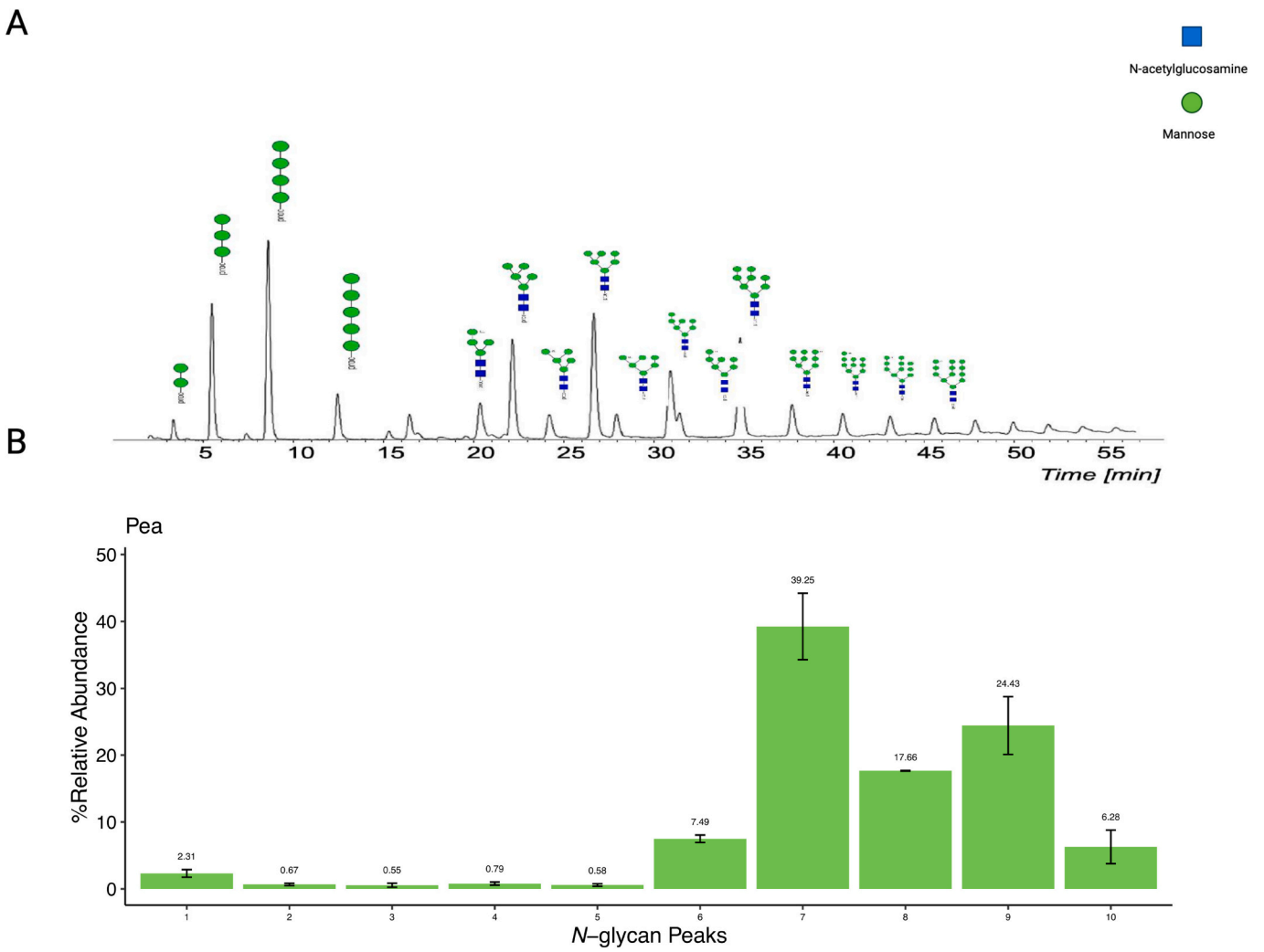

Fig. 5. Distinct *N*-glycan structures from pea glycoprotein and their relative abundance determined by peak areas from the FLD chromatogram. HILIC-HPLC with a fluorescence detector paired with QTOF-MS/MS produced chromatograms and determined structures and abundance for procainamide-labeled *N*-glycans from pea protein. A total of 10 peaks were identified corresponding to 10 distinct *N*-glycan structures. *N*-glycan structures for low abundant peaks not shown.

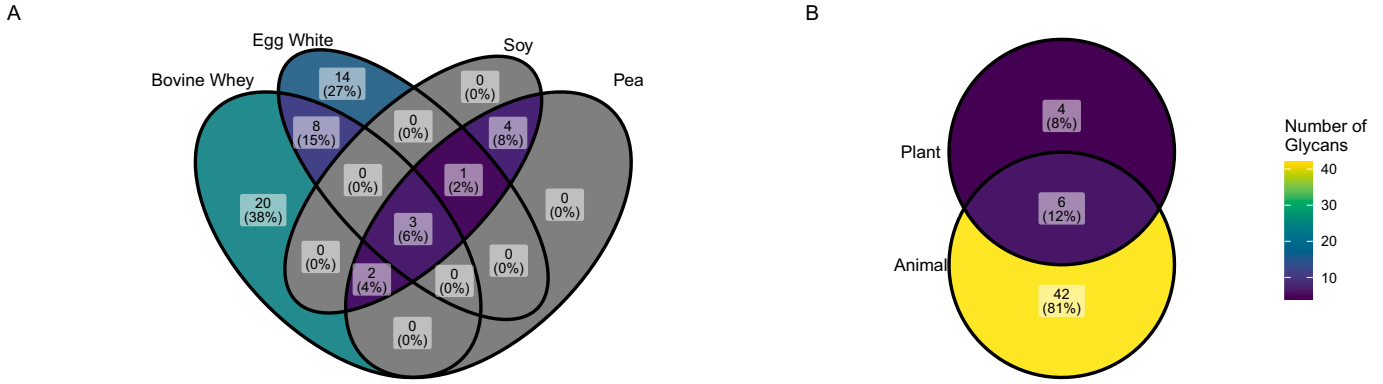

Fig. 6. Some *N*-glycan structures are unique, and others are shared between glycoproteins and glycoprotein sources as determined by HPLC-HILIC-FLD-QTOF-MS/MS. (A) Comparison of *N*-glycan structures between all glycoprotein sources determined by HPLC-QTOF-MS/MS. (B) Comparison of *N*-glycan structures between animal and plant sources.

The determination of the *N*-glycome for each of the four protein ingredients identified consistent findings in *N*-glycan architecture congruent with a broader understanding of *N*-glycan biosynthesis. Previous studies examining the *N*-glycome of bovine whey have consistently identified complex structures containing sialic acids and fucose (Nwosu et al., 2012; Valk-Weeber, Deelman-Driessen, et al., 2020; Valk-Weeber, Eshuis-de Ruiter, et al., 2020; van Leeuwen et al., 2012), which is consistent with our findings. Other work that has characterized the *N*-glycome for soy protein allergens are also in agreement with our findings of primarily oligomannosidic *N*-glycan structures (Li et al., 2016),

with some limited incorporation of monosaccharides such as xylose and *N*-glycan core fucosylation (Lu et al., 2022; Zhu et al., 2018). Minor differences with the reported literature can most likely be attributed to differences in methodologies. The identification of the egg white *N*-glycome is more limited, with most studies examining the egg *N*-glycome focusing on species that are not widely regarded as food sources (Sanes et al., 2019; Suzuki et al., 2004, 2009), or they have examined the egg yolk *N*-glycome from different animals (Kayılı, 2021; Roth et al., 2010). To our knowledge, this is the first report of the hen egg white and pea *N*-glycomes.

One limitation of the present work is that the method used here is not as sensitive as other methods to elucidate *N*-glycan structures, which may underestimate the diversity of *N*-glycan structures. However, HPLC-HILIC-FID-QTOF-MS/MS provides more consistent data for semi-quantitative analysis of *N*-glycans and is able to confidently identify bisecting *N*-glycan structures based on the procainamide labeling approach (Kayili, 2020). Further, we have not examined how and whether genetic or environmental determinants across breeds or strains of livestock or crops affect *N*-glycosylation, though there is evidence that free oligosaccharides and endogenous glycosidases found in bovine milk can vary (Robinson et al., 2019; Sunds et al., 2021), and the *N*-glycome of human milk is subject to physiological and genetic variation (Barboza et al., 2012; Smilowitz et al., 2013). Thus while there may be additional and unappreciated variation beyond the present work, when these protein sources are used in food manufacturing, their inclusion is in a form comparable to the substrates examined here.

The identification of the *N*-glycome of dietary glycoprotein sources is an important contribution to the developing study of how *N*-glycan composition can shape the gut microbiome. Studies have highlighted the ability of beneficial gut microbes, such as *B. infantis*, to metabolize *N*-glycans as substrates *in vitro* (Karav et al., 2016) and *in vivo* (Karav et al., 2019). Additional evidence reveals that particular strains show additional specialization to *N*-glycan utilization with a concurrent fitness advantage relative to other *B. infantis* strains *in vivo* (Barratt et al., 2022). It is likely that the observed differences in the complexity and decoration of *N*-glycans impact the human gut microbiome in different ways, however further studies are needed to elucidate how these differences affect the gut microbiome.

Funding

This work was made possible by funding from the University of Nevada, Reno Department of Nutrition; the University of Nevada, Reno College of Agriculture, Biotechnology, and Natural Resources; the Nevada Agriculture Experimental Station; and the University of Nevada, Reno Office of the Vice President for Research and Innovation. This work is also supported by a New Investigator Seed Grant from the USDA National Institute of Food and Agriculture, Grant #13385133.

CRediT authorship contribution statement

Matthew Bolino: Writing – review & editing, Writing – original draft, Visualization, Validation, Investigation, Formal analysis, Data curation, Conceptualization. **İzzet Avcı:** Writing – review & editing, Writing – original draft, Visualization, Methodology, Formal analysis. **Hacı Mehmet Kayili:** Writing – review & editing, Writing – original draft, Visualization, Resources, Methodology, Investigation. **Hatice Duman:** Writing – review & editing, Writing – original draft, Visualization, Formal analysis, Data curation. **Bekir Salih:** Supervision, Methodology, Investigation. **Sercan Karav:** Writing – review & editing, Writing – original draft, Supervision, Project administration, Methodology, Investigation, Conceptualization. **Steven A. Frese:** Writing – review & editing, Writing – original draft, Visualization, Supervision, Project administration, Methodology, Investigation, Funding acquisition, Data curation, Conceptualization.

Declaration of competing interest

The authors declare the following financial interests/personal relationships which may be considered as potential competing interests: Steven Frese reports financial support was provided by the United States Department of Agriculture's National Institute of Food and Agriculture. The other authors have no known competing financial interests have no known competing financial interests or personal relationships that could have appeared to influence the work reported in this paper.

Appendix A. Supplementary data

Supplementary data to this article can be found online at https://doi.org/10.1016/j.fochx.2024.102025.

Data availability

Data will be made available on request.

References

Aebi, M., Bernasconi, R., Clerc, S., & Molinari, M. (2010). N-glycan structures: Recognition and processing in the ER. *Trends in Biochemical Sciences, 35*(2), 74–82. https://doi.org/10.1016/j.tibs.2009.10.001

Anderson, M. J. (2001). A new method for non-parametric multivariate analysis of variance. *Austral Ecology, 26*(1), 32–46. https://doi.org/10.1111/j.1442-9993.2001.01070.pp.x

Barboza, M., Pinzon, J., Wickramasinghe, S., Froehlich, J. W., Moeller, I., Smilowitz, J. T., … Lebrilla, C. B. (2012). Glycosylation of human milk lactoferrin exhibits dynamic changes during early lactation enhancing its role in pathogenic bacteria-host interactions *. *Molecular & Cellular Proteomics, 11*(6). https://doi.org/10.1074/mcp.M111.015248

Barratt, M. J., Nuzhat, S., Ahsan, K., Frese, S. A., Arzamasov, A. A., Sarker, S. A., … Gordon, J. I. (2022). Bifidobacterium infantis treatment promotes weight gain in Bangladeshi infants with severe acute malnutrition. *Science Translational Medicine, 14*(640), Article eabk1107. https://doi.org/10.1126/scitranslmed.abk1107

Bieberich, E. (2014). Synthesis, processing, and function of N-glycans in N-glycoproteins. *Advances in Neurobiology, 9*, 47–70. https://doi.org/10.1007/978-1-4939-1154-7_3

Bray, J. R., & Curtis, J. T. (1957). An ordination of the upland forest communities of southern Wisconsin. *Ecological Monographs, 27*(4), 326–349. https://doi.org/10.2307/1942268

Briliūtė, J., Urbanowicz, P. A., Luis, A. S., Baslé, A., Paterson, N., Rebello, O., … Crouch, L. I. (2019). Complex N-glycan breakdown by gut bacteroides involves an extensive enzymatic apparatus encoded by multiple co-regulated genetic loci. *Nature Microbiology, 4*(9), 1571–1581. https://doi.org/10.1038/s41564-019-0466-x

Castilho, A., Gattinger, P., Grass, J., Jez, J., Pabst, M., Altmann, F., Gorfer, M., Strasser, R., & Steinkellner, H. (2011). N-glycosylation engineering of plants for the biosynthesis of glycoproteins with bisected and branched complex N-glycans. *Glycobiology, 21*(6), 813–823. https://doi.org/10.1093/glycob/cwr009

Ceroni, A., Maass, K., Geyer, H., Geyer, R., Dell, A., & Haslam, S. M. (2008). Glycoworkbench: A tool for the computer-assisted annotation of mass spectra of glycans. *Journal of Proteome Research, 7*(4), 1650–1659. https://doi.org/10.1021/pr7008252

Crouch, L. I., Urbanowicz, P. A., Baslé, A., Cai, Z.-P., Liu, L., Voglmeir, J., … Bolam, D. N. (2022). Plant N-glycan breakdown by human gut bacteroides. *Proceedings of the National Academy of Sciences of the United States of America, 119*(39), Article e2208168119. https://doi.org/10.1073/pnas.2208168119

Dallas, D. C., Martin, W. F., Strum, J. S., Zivkovic, A. M., Smilowitz, J. T., Underwood, M. A., … German, J. B. (2011). N-linked glycan profiling of mature human milk by high-performance microfluidic chip liquid chromatography time-of-flight tandem mass spectrometry. *Journal of Agricultural and Food Chemistry, 59*(8), 4255–4263. https://doi.org/10.1021/jf104681p

Dixon, P. (2003). VEGAN, a package of R functions for community ecology. *Journal of Vegetation Science, 14*(6), 927–930. https://doi.org/10.1111/j.1654-1103.2003.tb02228.x

Doubet, S., & Albersheim, P. (1992). CarbBank. *Glycobiology, 2*(6), 505. https://doi.org/10.1093/glycob/2.6.505

Fernández-Tejada, A., Brailsford, J., Zhang, Q., Shieh, J.-H., Moore, M. A. S., & Danishefsky, S. J. (2015). Total synthesis of glycosylated proteins. *Topics in Current Chemistry, 362*, 1–26. https://doi.org/10.1007/128_2014_622

Helenius, A., & Aebi, M. (2004). Roles of N-linked glycans in the endoplasmic reticulum. *Annual Review of Biochemistry, 73*, 1019–1049. https://doi.org/10.1146/annurev.biochem.73.011303.073752

Karav, S., de MouraBell, J. M. L. N., le Parc, A., Liu, Y., Mills, D. A., Block, D. E., & Barile, D. (2015). Characterizing the release of bioactive N-glycans from dairy products by a novel endo-β-N-acetylglucosaminidase. *Biotechnology Progress, 31*(5), 1331–1339. https://doi.org/10.1002/btpr.2135

Karav, S., Casaburi, G., Arslan, A., Kaplan, M., Sucu, B., & Frese, S. (2019). N-glycans from human milk glycoproteins are selectively released by an infant gut symbiont in

vivo. *Journal of Functional Foods, 61*, Article 103485. https://doi.org/10.1016/j.jff.2019.103485

Karav, S., le Parc, A., Nobrega, L., de Moura Bell, J. M., Frese, S. A., Kirmiz, N., … Mills, D. A. (2016). Oligosaccharides released from milk glycoproteins are selective growth substrates for infant-associated bifidobacteria. *Applied and Environmental Microbiology, 82*(12), 3622–3630. https://doi.org/10.1128/AEM.00547-16

Karav, S., Parc, A. L., de Moura Bell, J. M. L. N., Rouquié, C., Mills, D. A., Barile, D., & Block, D. E. (2015). Kinetic characterization of a novel endo-β-N-acetylglucosaminidase on concentrated bovine colostrum whey to release bioactive glycans. *Enzyme and Microbial Technology, 77*, 46–53. https://doi.org/10.1016/j.enzmictec.2015.05.007

Kayili, H. M. (2020). Identification of bisecting *N*-glycans in tandem mass spectra using a procainamide labeling approach for in-depth *N*-glycan profiling of biological samples. *International Journal of Mass Spectrometry, 457*, Article 116412. https://doi.org/10.1016/j.ijms.2020.116412

Kayılı, H. M. (2021). In-depth profiling of N-glycans isolated from ostrich egg white and yolk glycoproteomes by HPLC-HILIC-FLD-MS/MS. *Adıyaman University Journal of Science, 11*(1), 191–204.

Kayili, H. M., & Salih, B. (2021). N-glycan profiling of glycoproteins by hydrophilic interaction liquid chromatography with fluorescence and mass spectrometric detection. *Journal of Visualized Experiments: JoVE, 175*. https://doi.org/10.3791/62751

Koropatkin, N. M., Cameron, E. A., & Martens, E. C. (2012). How glycan metabolism shapes the human gut microbiota. *Nature Reviews Microbiology, 10*(5), 5. https://doi.org/10.1038/nrmicro2746

Kruskal, W. H., & Wallis, W. A. (1952). Use of ranks in one-criterion variance analysis. *Journal of the American Statistical Association, 47*(260), 583–621. https://doi.org/10.1080/01621459.1952.10483441

van Leeuwen, S. S., Schoemaker, R. J. W., Timmer, C. J. A. M., Kamerling, J. P., & Dijkhuizen, L. (2012). N- and O-glycosylation of a commercial bovine whey protein product. *Journal of Agricultural and Food Chemistry, 60*(51), 12553–12564. https://doi.org/10.1021/jf304000b

Li, L., Wang, C., Qiang, S., Zhao, J., Song, S., Jin, W., … Wang, Z. (2016). Mass spectrometric analysis of N-glycoforms of soybean allergenic glycoproteins separated by SDS-PAGE. *Journal of Agricultural and Food Chemistry, 64*(39), 7367–7376. https://doi.org/10.1021/acs.jafc.6b02773

Lu, Y., Sun, L., Li, C., Wang, X., Li, W., Zhao, T., Huang, L., & Wang, Z. (2022). Comparative mass spectrometry analysis of *N*-glycans from the glycoproteins of eight allergy-inducing plants. *Food Chemistry, 384*, Article 132440. https://doi.org/10.1016/j.foodchem.2022.132440

Molinari, M. (2007). N-glycan structure dictates extension of protein folding or onset of disposal. *Nature Chemical Biology, 3*(6), 6. https://doi.org/10.1038/nchembio880

Nwosu, C. C., Aldredge, D. L., Lee, H., Lerno, L. A., Zivkovic, A. M., German, J. B., & Lebrilla, C. B. (2012). Comparison of the human and bovine milk N-glycome via high-performance microfluidic chip liquid chromatography and tandem mass spectrometry. *Journal of Proteome Research, 11*(5), 2912–2924. https://doi.org/10.1021/pr300008u

Parc, A. L., Karav, S., de Moura Bell, J. M. L. N., Frese, S. A., Liu, Y., Mills, D. A., … Barile, D. (2015). A novel endo-β-N-acetylglucosaminidase releases specific N-glycans depending on different reaction conditions. *Biotechnology Progress, 31*(5), 1323–1330. https://doi.org/10.1002/btpr.2133

Pedrazzini, E., Caprera, A., Fojadelli, I., Stella, A., Rocchetti, A., Bassin, B., Martinoia, E., & Vitale, A. (2016). The Arabidopsis tonoplast is almost devoid of glycoproteins with complex N-glycans, unlike the rat lysosomal membrane. *Journal of Experimental Botany, 67*(6), 1769–1781. https://doi.org/10.1093/jxb/erv567

Robinson, R. C., Poulsen, N. A., Colet, E., Duchene, C., Larsen, L. B., & Barile, D. (2019). Profiling of aminoxyTMT-labeled bovine milk oligosaccharides reveals substantial variation in oligosaccharide abundance between dairy cattle breeds. *Scientific Reports, 9*(1), 5465. https://doi.org/10.1038/s41598-019-41956-x

Roth, Z., Parnes, S., Wiel, S., Sagi, A., Zmora, N., Chung, J. S., & Khalaila, I. (2010). N-glycan moieties of the crustacean egg yolk protein and their glycosylation sites. *Glycoconjugate Journal, 27*(1), 159–169. https://doi.org/10.1007/s10719-009-9268-3

Sanes, J. T., Hinou, H., Lee, Y. C., & Nishimura, S.-I. (2019). Glycoblotting of egg white reveals diverse N-glycan expression in quail species. *Journal of Agricultural and Food Chemistry, 67*(1), 531–540. https://doi.org/10.1021/acs.jafc.8b04782

Shannon, C. E. (1948). A mathematical theory of communication. *The Bell System Technical Journal, 27*(3), 379–423. The Bell System Technical Journal https://doi.org/10.1002/j.1538-7305.1948.tb01338.x.

Skropeta, D. (2009). The effect of individual N-glycans on enzyme activity. *Bioorganic & Medicinal Chemistry, 17*(7), 2645–2653. https://doi.org/10.1016/j.bmc.2009.02.037

Smeuninx, B., Greig, C. A., & Breen, L. (2020). Amount, source and pattern of dietary protein intake across the adult lifespan: A cross-sectional study. *Frontiers in Nutrition, 7*, 25. https://doi.org/10.3389/fnut.2020.00025

Smilowitz, J. T., Totten, S. M., Huang, J., Grapov, D., Durham, H. A., Lammi-Keefe, C. J., … German, J. B. (2013). Human milk secretory immunoglobulin a and lactoferrin N-glycans are altered in women with gestational diabetes mellitus123. *The Journal of Nutrition, 143*(12), 1906–1912. https://doi.org/10.3945/jn.113.180695

Stanley, P., Taniguchi, N., & Aebi, M. (2015). N-Glycans (Eds.). In A. Varki, R. D. Cummings, J. D. Esko, P. Stanley, G. W. Hart, M. Aebi, … P. H. Seeberger (Eds.), *Essentials of glycobiology*. Cold Spring Harbor Laboratory Press (3rd ed.). Chapter 9. http://www.ncbi.nlm.nih.gov/books/NBK453020/.

Strasser, R. (2016). Plant protein glycosylation. *Glycobiology, 26*(9), 926–939. https://doi.org/10.1093/glycob/cww023

Sunds, A. V., Roland, I. S., Sundekilde, U. K., Thesbjerg, M. N., Robinson, R., Bunyatratchata, A., … Poulsen, N. A. (2021). Naturally occurring glycosidases in milk from native cattle breeds: Activity and consequences on free and protein bound-glycans. *Metabolites, 11*(10), 662. https://doi.org/10.3390/metabo11100662

Suzuki, N., Laskowski, M., & Lee, Y. C. (2004). Phylogenetic expression of galα1-4Gal on avian glycoproteins: Glycan differentiation inscribed in the early history of modern birds. *Proceedings of the National Academy of Sciences, 101*(24), 9023–9028. https://doi.org/10.1073/pnas.0402822101

Suzuki, N., Su, T.-H., Wu, S.-W., Yamamoto, K., Khoo, K.-H., & Lee, Y. C. (2009). Structural analysist of N-glycans from gull egg white glycoproteins and egg yolk IgG. *Glycobiology, 19*(7), 693–706. https://doi.org/10.1093/glycob/cwp025

Takada, H., Katoh, T., & Katayama, T. (2020). Sialylated O -glycans from hen egg white ovomucin are decomposed by mucin-degrading gut microbes. *Journal of Applied Glycoscience, 67*(2), 31. https://doi.org/10.5458/jag.jag.JAG-2019_0020

Valk-Weeber, R. L., Deelman-Driessen, C., Dijkhuizen, L., Eshuis-de Ruiter, T., & van Leeuwen, S. S. (2020). In depth analysis of the contribution of specific glycoproteins to the overall bovine whey N-linked glycoprofile. *Journal of Agricultural and Food Chemistry, 68*(24), 6544–6553. https://doi.org/10.1021/acs.jafc.0c00959

Valk-Weeber, R. L., Eshuis-de Ruiter, T., Dijkhuizen, L., & van Leeuwen, S. S. (2020). Quantitative analysis of bovine whey glycoproteins using the overall *N*-linked whey glycoprofile. *International Dairy Journal, 110*, Article 104814. https://doi.org/10.1016/j.idairyj.2020.104814

Wang, P., Wang, H., Gai, J., Tian, X., Zhang, X., Lv, Y., & Jian, Y. (2017). Evolution of protein N-glycosylation process in golgi apparatus which shapes diversity of protein N-glycan structures in plants, animals and fungi. *Scientific Reports, 7*, 40301. https://doi.org/10.1038/srep40301

Zhu, Y., Yan, M., Lasanajak, Y., Smith, D. F., & Xuezheng, S. (2018). Large scale preparation of high mannose and paucimannose N-glycans from soybean proteins by oxidative release of natural glycans (ORNG). *Carbohydrate Research, 464*, 19–27. https://doi.org/10.1016/j.carres.2018.05.002

Zivkovic, A. M., German, J. B., Lebrilla, C. B., & Mills, D. A. (2011). Human milk glycobiome and its impact on the infant gastrointestinal microbiota. *Proceedings of the National Academy of Sciences, 108*, 4653–4658. https://doi.org/10.1073/pnas.1000083107. Supplement 1.